

TIDALLY INDUCED BROWN DWARF AND PLANET FORMATION IN CIRCUMSTELLAR DISCS

INGO THIES¹, PAVEL KROUPA¹, SIMON P. GOODWIN², DIMITRIOS STAMATELLOS³, ANTHONY P. WHITWORTH³

Draft version October 24, 2018

ABSTRACT

Most stars are born in clusters and the resulting gravitational interactions between cluster members may significantly affect the evolution of circumstellar discs and therefore the formation of planets and brown dwarfs. Recent findings suggest that tidal perturbations of typical circumstellar discs due to close encounters may inhibit rather than trigger disc fragmentation and so would seem to rule out planet formation by external tidal stimuli. However, the disc models in these calculations were restricted to disc radii of 40 AU and disc masses below $0.1 M_{\odot}$. Here we show that even modest encounters can trigger fragmentation around 100 AU in the sorts of massive ($\sim 0.5 M_{\odot}$), extended (≥ 100 AU) discs that are observed around young stars. Tidal perturbation alone can do this, no disc-disc collision is required. We also show that very-low-mass binary systems can form through the interaction of objects in the disc. In our computations, otherwise non-fragmenting massive discs, once perturbed, fragment into several objects between about 0.01 and $0.1 M_{\odot}$, i.e., over the whole brown dwarf mass range. Typically these orbit on highly eccentric orbits or are even ejected. While probably not suitable for the formation of Jupiter- or Neptune-type planets, our scenario provides a possible formation mechanism for brown dwarfs and very massive planets which, interestingly, leads to a mass distribution consistent with the canonical substellar IMF. As a minor outcome, a possible explanation for the origin of misaligned extrasolar planetary systems is discussed.

Subject headings: binaries: general — open clusters and associations: general — stars: formation — stars: low-mass, brown dwarfs — planetary systems: protoplanetary disks —

1. INTRODUCTION

The origin of brown dwarfs (BDs, to which we also include very low-mass stars $< 0.1 M_{\odot}$) as well as the formation of massive exoplanets is contentious. The most common idea is that BDs form like stars, and planets form by accretion onto a core formed from dust conglomeration within a circumstellar disc. However, there is increasing evidence that an alternative formation scenario for BDs and, possibly, some of the most massive exoplanets is required. BDs differ from low-mass stars in several ways. Firstly, there is the ‘brown dwarf desert’ – a lack of BD companions to stars, especially at separations below about 30 AU within which companion planets and stars are common. In addition, the properties of BD-BD binaries are very different from star-star binaries, showing a significant lack of systems wider than ≈ 20 AU beyond which most stellar binaries are found. Furthermore, while typically every second star is a binary system only every fifth BD is a binary. Clearly we must ask ourselves why stars and BDs are so different if they form by the same mechanism. Indeed, in order to numerically set-up a realistic stellar and BD population, stars and BDs need to be according to different algorithmic pairing rules Kroupa et al. (2003). In other words, they follow different formation channels.

The fragmentation of extended circumstellar discs is one of the most promising alternatives to the standard scenario of star-like formation for BDs (Goodwin & Whitworth 2007). Research on circumstellar disc evolution has made great progress in recent years, but there are still many unanswered questions (Papaloizou & Terquem 2006; Henning

2008; Hillenbrand 2008). One issue that has gained surprisingly little attention in the past is the role of gravitational interactions between the disc and passing stars within the young host stellar cluster. Since stars are generally born in clusters (Forgan & Rice 2009), rather than as isolated objects, star-disc and disc-disc interactions (Boffin et al. 1998; Watkins et al. 1998a; Pfalzner et al. 2005; Thies et al. 2005) probably play an important role for the dynamical evolution of such discs and thus for massive planet and BD formation through fragmentation of the discs.

For a typical open star cluster hosting about 1000 stars within a half-mass radius of 0.5 pc, encounters closer than 500 AU will happen approximately every 10 Myr (Thies et al. 2005). They are even more frequent in denser clusters in which are thought to form at least half of the stars in the Galaxy. Encounters in star clusters are therefore expected to play a significant role in the evolution of extended discs of several 100 AU radii.

The formation of planets through core accretion is typically expected to happen within the innermost 100 AU of a circumstellar disc (Hillenbrand 2008), although there are many unanswered questions especially concerning the very first stages of core accretion (Henning 2008). Fragmentation has been proposed as an alternative way to form the most massive gas giant planets by Mayer et al. (2002); Boss (1997, 2004, 2006). In recent years, however, there has been a growing consensus that disc fragmentation cannot produce gas giant planets in the inner regions of discs for two reasons: (1) heating from the central star stabilizes the innermost regions and thus inhibits fragmentation, and (2) these regions cannot cool fast enough to allow temporary gas clumps to collapse (Lodato et al. 2007; Stamatellos & Whitworth 2008; Cai et al. 2010). This picture changes greatly beyond about 100 AU where cooling becomes sufficiently efficient for gravitational collapse to occur. Consequently, disc frag-

¹ Argelander-Institut für Astronomie (Sternwarte), Universität Bonn, Auf dem Hügel 71, D-53121 Bonn, Germany

² Department of Physics and Astronomy, University of Sheffield, Sheffield S3 7RH, UK

³ School of Physics & Astronomy, Cardiff University, Cardiff CF24 3AA, UK

mentation has been proposed as an alternative mechanism for the formation of BDs (Whitworth & Stamatellos 2006; Goodwin & Whitworth 2007). Most of these investigations, however, assume that the disc evolves in isolation.

Star-disc and disc-disc collisions have been investigated in previous studies (Boffin et al. 1998; Watkins et al. 1998a,b) but without a realistic treatment of the radiative heat transfer in the disc. From SPH computations Forgan & Rice (2009) deduce that close encounters inhibit fragmentation in typical protoplanetary discs (assuming an initial radius of 40 AU) rather than inducing it. In contrast to that, a recent study of disc-disc collisions (Shen et al. 2010) has, however, shown that the direct compression of gas by the close encounters of stars hosting massive extended discs (disc mass $\approx 0.5 M_{\odot}$, disc radius ≈ 1000 AU), may trigger the formation of sub-stellar companions. However such massive, extended discs are probably short-lived (Eisner & Carpenter 2006) (in contrast to typical protoplanetary discs which are about ten times smaller and less massive), so that pairwise interactions of two discs of this kind are expected to be rare. The purely gravitational interaction of a low-mass star with no (or only a small) protoplanetary disc with a star hosting a massive disc would be much more likely. Although even these encounters may probably account for only a fraction of all BDs, especially in loose associations like Taurus-Auriga, they provide an additional channel of forming BDs out of discs that would otherwise probably dissolve without ever fragmenting. In this paper we address this issue. In Section 2, besides an estimate of the encounter probability, the model of the circumstellar disc is described. Section 3 depicts the computational methods and gives an overview of the model parameters studied in this work. The results are then presented in Section 4 and discussed in Section 5

2. MODEL BASICS

2.1. Encounter probability

The likelihood of a close stellar encounter with an impact parameter b depends on the stellar density of the star-forming environment and the impact parameter itself. The encounter event is then further characterized by the relative velocity of the two stars and thus the eccentricity of the path. The consequences on the circumstellar disc further depend on the mass of the perturber and the host star (i.e., the ratio of binding energy and magnitude of the perturbation) and the inclination of the disc plane wrt. the plane of the encounter hyperbola.

Stars can be born in a variety of environments from low-density groups like Taurus-Auriga (about 300 stars distributed in groups, each being <1 pc in radius and containing about a few dozen stars) up to ONC-type clusters (thousands of stars within 0.5 pc) or even in more massive and dense clusters (Kroupa 2005). An estimate of the encounter probability has been derived assuming a Plummer star cluster model of half-mass radius, $r_{1/2}$, total mass M_{tot} , and an average stellar mass, M_{\star} . Note that two other radial scales are also often used to describe a Plummer model: the Plummer radius, $r_{\text{Pl}} = \sqrt{2^{2/3} - 1} r_{1/2} \approx 0.766 r_{1/2}$, and the gravitational scale radius, $r_{\text{grav}} \approx 2.602 r_{1/2} \approx 3.395 r_{\text{Pl}}$. From Thies et al. (2005), Section 1.3, the expected time, t_{enc} , between two encounters within an encounter parameter, b , can be obtained from the characteristic crossing time t_{cr} ,

$$\frac{t_{\text{cr}}}{\text{Myr}} = 83 \left(\frac{M_{\text{tot}}}{M_{\odot}} \right)^{-1/2} \left(\frac{r_{1/2}}{\text{pc}} \right)^{3/2}, \quad (1)$$

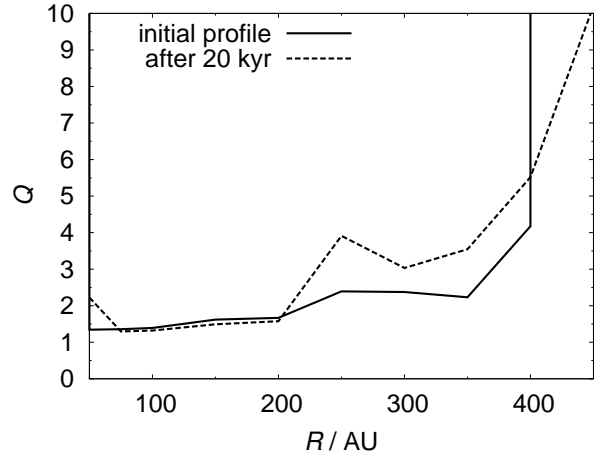


FIG. 1.— The Toomre parameter Q as a function of the radius from the central star for both the initial disc setup (solid line) and the settled disc after 20 kyr (dashed line). The profiles of both disc stages are nearly identical below about 200 AU while Q is slightly larger (i.e. the disc is more stable) between 200 AU and 400 AU, the outer rim of the initial disc. The region within 50 AU is skipped since it is initially partially void.

and the average number, n_{enc} , of encounter parameters below b , for a given number of stars, N ,

$$n_{\text{enc}}(< b) = N \frac{b^2}{r_{\text{grav}}^2}. \quad (2)$$

t_{enc} is approximately given by

$$\frac{t_{\text{enc}}}{\text{Myr}} = \frac{2.4 \times 10^{13}}{N} \left(\frac{M_{\text{tot}}}{M_{\odot}} \right)^{-1/2} \left(\frac{r_{1/2}}{\text{pc}} \right)^{7/2} \left(\frac{b}{\text{AU}} \right)^{-2}. \quad (3)$$

It has to be noted that the actual periastron distance, r_{peri} , is always (and sometimes significantly) smaller than b due to gravitational focusing. The relation between r_{peri} and b for a given eccentricity, e , is

$$r_{\text{peri}} = \sqrt{\frac{e-1}{e+1}} b. \quad (4)$$

For an ONC-type cluster with $N = 7500$, an average star mass $M_{\star} = 0.5 M_{\odot}$, a total mass $M_{\text{tot}} = 10000 M_{\odot}$ (i.e., 30% of the mass consists of stars and the rest of gas, see Kroupa et al. 2001), and a half-mass radius of $r_{1/2} = 0.5$ pc we find that encounters below 500 AU occur on average every 11 million years. If a massive extended disc exists for about 1 Myr this means that about 9 per cent of all discs of this type will suffer such an encounter. See also Thies et al. (2005).

2.2. Disc model

The initial conditions for the disc are taken from Stamatellos & Whitworth (2008, 2009a). The disc model has a power law profile for temperature, T , and surface density, Σ from Stamatellos & Whitworth (2008), both as a function of the distance, R , from the central star,

$$\Sigma(R) = \Sigma_0 \left(\frac{R}{\text{AU}} \right)^{-q_{\Sigma}}, \quad (5)$$

$$T(R) = \left[T_0^2 \left(\frac{R}{\text{AU}} \right)^{-2q_T} + T_{\infty}^2 \right]^{1/2}, \quad (6)$$

where $q_\Sigma = 1.75$, $q_T = 0.5$, and $T_0 = 300$ K. Σ_0 is chosen corresponding to a disc mass of 0.48 and 0.50 M_\odot (see Table 1), i.e., $\Sigma_0 = 8.67 \times 10^4$ g cm $^{-2}$ and $\Sigma_0 = 9.03 \times 10^4$ g cm $^{-2}$, respectively. $T_\infty = 10$ K is a background temperature to account for the background radiation from other stars within the host cluster. This configuration leads to an initial Toomre stability parameter, Q , (Toomre 1964) between 1.3 and 1.4 between about 100 and 400 AU, leading to weak spiral density patterns but not to fragmentation. Q is given by

$$Q = \frac{c_s \kappa}{\pi G \Sigma} \quad (7)$$

with c_s being the sound speed, and κ being the epicyclic frequency which can be, at least roughly, approximated by the Keplerian orbital frequency. The radiation of the perturber is included in the same way as that of the central star, assuming a mass-to-luminosity relation of $L \propto M^4$ for low-mass stars. However, as long as the perturber is no more than about 0.5 M_\odot , corresponding to an early M-type or late K-type main sequence star, its influence on disc evolution is very small.

The disc is initially populated by SPH particles between 40 and 400 AU. Before starting the actual encounter computation the disc is allowed to “settle” for about 20 000 years (i.e., about two orbits at the outer rim) to avoid artefacts from the initial distribution function. During this settling the disc smears out at the inner and the outer border extending its radial range from a few AU up to $\gtrsim 500$ AU, eventually stabilising. The Q value is slightly increased beyond 200 AU relative to the initial setting while remaining largely unchanged below this radius, as can be seen in Figure 1. The actual surface density after the settling is therefore slightly smaller and thus the disc slightly more stable than in the initial setup. Any self-fragmentation of the unperturbed disc would have happened during the settling time when the Toomre parameter is lowest.

3. METHODS

3.1. Smoothed particle hydrodynamics (SPH)

All computations were performed by using the well-tested DRAGON SPH code by Goodwin et al. (2004) including the radiative transfer extension by Stamatellos et al. (2007b). Most of the numerical parameter settings have been adopted from Stamatellos et al. (2007a); Stamatellos & Whitworth (2009a). Gravitationally collapsing clumps are treated by sink particles which form if the volume density exceeds 10^{-9} g cm $^{-3}$, and the clump is bound. The sink radius is 1 AU, in accordance with the studies mentioned above and in agreement with the local Jeans criterion. In addition, the central star and the perturbing star are both represented by sink particles.

There are ongoing discussions whether fragmentation can be triggered artificially due to the numerical behaviour of SPH and grid-based hydrocodes. Hubber et al. (2006) find that smoothed particle hydrodynamics (SPH) does not suffer from artificial fragmentation. However, Nelson (2006) suggest that SPH may artificially enhance fragmentation due to a pressure-underestimation if the smoothing radius, h , is considerably larger than about 1/4 of a vertical scale height of a circumstellar disc. Stamatellos & Whitworth (2009b) show that this criterion is fulfilled for 150,000 or more particles, for the types of disc studied in this paper.

Commerçon et al. (2008) have performed calculations of fragmenting protostellar clouds with the adaptive mesh refinement (AMR) code RAMSES and the SPH code DRAGON

(which we have been using for this study) and compared the results at different resolutions given by the number N of grid cells and particles, respectively. For about $N = 5 \times 10^5$ cells/particles fragmentation in both codes appeared nearly equal. With $N = 2 \times 10^5$ the results were very similar to the high-resolution AMR computations while being still acceptable for many purposes at $N = 1 \times 10^5$. Stamatellos & Whitworth (2009b) briefly review the resolution criteria with respect to their models using 150 000 in that paper and 250 000 to 400 000 particles earlier (Stamatellos & Whitworth 2009a).

The three most important resolution criteria are the resolution of the local Jeans mass, M_J , (and thus the Jeans length), the local Toomre mass and the vertical scale height of the disc. In particular, the local Jeans mass,

$$M_J = \frac{4\pi^{5/2}}{24} \frac{c_s^3}{\sqrt{G^3 \rho}}, \quad (8)$$

must be resolved by at least a factor of $2 \times N_{\text{neigh}} = 100$, corresponding to 0.5 M_J for the 100,000 particle discs and 0.2 M_J for the 250,000 particle discs. Since the global disc setup as well as the evolution after the perturbation (Section 4) is quite similar to that used by (Stamatellos & Whitworth 2009b), as similar range of Jeans masses of the forming clumps, i.e., ~ 2 –20 M_J , can be reasonably assumed for our models and has actually been tested for the models E/X002 and E/X009 for all forming objects. The minimum M_J during the clump formation is typically between 4 and 6 M_J and does never go below about 2 M_J . Therefore, M_J is resolved by a safe factor of at least 4 in the low-resolution case and 10 in the high-resolution case. Accordingly, the minimum Toomre mass of 2.5 M_J is adequately resolved as well as the vertical scale height (by at least a few smoothing lengths).

3.2. Radiative transfer model

In Thies et al. (2005) the possibility of fragmentation has been estimated via the Toomre criterion for both isothermal and adiabatic equations of state, both resulting in perturbed regions with highly unstable conditions ($Q < 1$). However, Toomre instability does not necessarily lead to actual fragmentation.

In realistic models of radiative transfer, such as the one used here, the thermal response of the gas to density changes is between near-isothermal in regions with efficient cooling (outside about 100–200 AU) and near-adiabatic in regions with long cooling times (the inner parts of the disc). Shen et al. (2010) have shown that direct disc-disc collisions may lead to fragmentation of massive extended discs at some 400 AU even for a “thick disc approximation”, i.e., the near-adiabatic case.

The Stamatellos et al. (2007b) method uses the density and the gravitational potential of each SPH particle to estimate an optical depth for each particle through which the particle cools and heats. The method takes into account compressional heating, viscous heating, radiative heating by the background, and radiative cooling. It performs well, in both the optically thin and optically thick regimes, and has been extensively tested by Stamatellos et al. (2007b). In particular it reproduces the detailed 3D results of Masunaga & Inutsuka (2000), Boss & Bodenheimer (1979), Boss & Myhill (1992), (Whitehouse & Bate 2006), and also the analytic results of Spiegel (1957). Additionally the code has been tested and

performs well in disc configurations as it reproduces the analytic results of Hubeny (1990).

The gas is assumed to be a mixture of hydrogen and helium. We use an equation of state by Black & Bodenheimer (1975); Masunaga et al. (1998); Boley et al. (2007) that accounts (1) for the rotational and vibrational degrees of freedom of molecular hydrogen, and (2) for the different chemical states of hydrogen and helium. We assume that ortho- and para-hydrogen are in equilibrium.

For the dust and gas opacity we use the parameterisation by Bell & Lin (1994), $\kappa(\rho, T) = \kappa_0 \rho^a T^b$, where κ_0 , a , b are constants that depend on the species and the physical processes contributing to the opacity at each ρ and T . The opacity changes due to ice mantle melting, the sublimation of dust, molecular and H^- contributions, are all taken into account.

3.3. Overview of Calculations

We have conducted thirteen SPH calculations using 100,000 and eight using 250,000 SPH particles (i.e., 21 models in total) corresponding to about nine CPU months in total on 16-core machines. The model identifiers that begin with an ‘‘E’’ or ‘‘F’’ refer to the low resolution models while the models with ‘‘X’’ or ‘‘Y’’ are the high resolution ones. Subsequent letters with identical numbers correspond to follow-up calculations (beginning at the moment of the closest encounter) with identical model settings. Due to the dynamical interaction of the parallel computing CPUs a slight random perturbation is imposed to the subsequent evolution such that the outcome differs within the statistical noise. The high resolution calculations are set up with parameters of preceding lower-resolution models that showed fragmentation. Therefore, the fact that all high resolution computations show fragmentation is due to the parameter selection. The low-resolution calculations are used as a parameter survey while the high resolution ones are follow-ups to selected low-resolution ones. Please note that not all non-fragmenting models are listed here but only those which represent the borders of the parameter space between fragmentation and no fragmentation.

We chose a $0.5 M_\odot$ perturbing star as a typical member of a star cluster (Kroupa 2001) for the majority of models, but we also performed calculations with perturbers down to $0.3 M_\odot$. The encounter orbit is slightly inclined ($i = 10^\circ$ against the initial disc plane) with varying eccentricities from $e = 1.1$ (near-parabolic) to $e = 2$ (hyperbolic), corresponding to a relative velocity of $0.4\text{--}2.7 \text{ km s}^{-1}$ at infinity. For these parameters the disc typically fragments to form a few very-low-mass stars and substellar-mass objects. A calculation with $e = 3$ has been performed but yielded no fragmentation. The same holds true for encounters at 600 AU or more. Depending on the eccentricity the calculations start 5000–10000 years before periastron to ensure a sufficiently low initial interaction. The calculations continue for 15 000 years after encounter for the models E/X/Y002 and at least 20 000 for the others. The masses and orbital radii of the objects formed in the calculation are determined at this time. After 15 000 years the accretion process of the objects has largely finished while dynamical evolution may still lead to major changes of the orbital parameters (and even to ejections of some bodies) if the calculations would have been continued over a longer time interval. For this reason, the orbital separations computed in this study have to be taken as a preliminary state.

It has to be noted that the orbit is altered slightly during the passage due to the transfer of mass and angular momen-

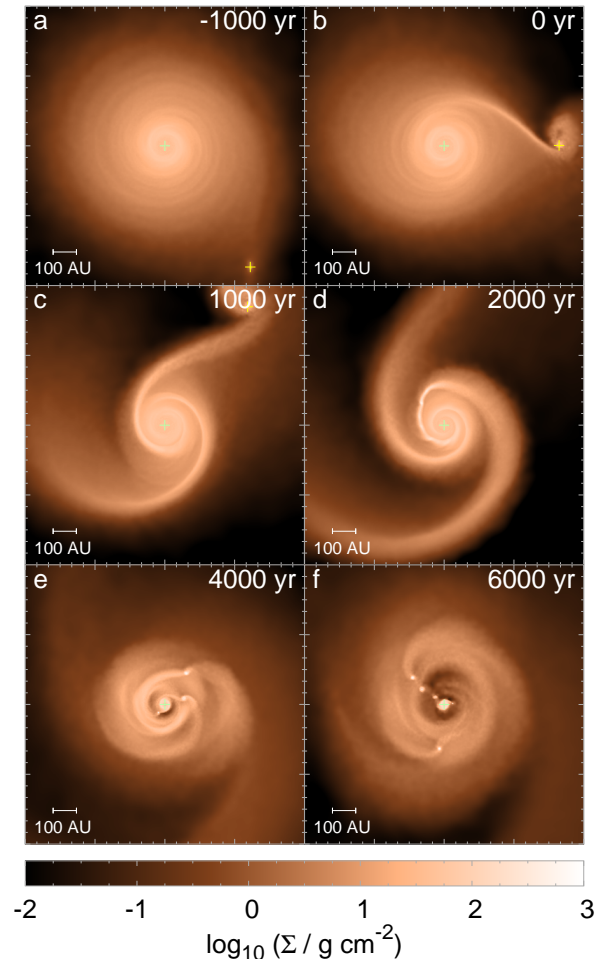


FIG. 2.— Snapshot of a circumstellar disc modelled with 250,000 SPH particles, around a Sun-type star being perturbed by a close star-star encounter (model X002, Table 1). The time stamp in each frame refers to the time of the encounter.

tum. Furthermore, since the encounter dissipates energy the post-encounter speed is typically lower than the pre-encounter speed and in some cases both stars may be captured in an eccentric binary (which actually happened to the companions 1a and 1b in calculation E003; see Table 1 and Figures 3 and 4). We found, however, that these effects are small.

4. RESULTS

4.1. General findings

As the unperturbed disc is marginally stable it does not fragment until the passage of the perturbing star. The first visible effects of a typical fly-by are the appearance of tidal arms and a mass transfer to the passing star (which acquires a small disc). About 2000–3000 years after the periastron passage parts of the tidal arms become gravitationally unstable, and spiral-shaped over-densities begin to form (see the snapshots from model X002 in Figure 2¹). Some of these continue to contract into a runaway collapse and form bound objects represented by sinks (see Section 3). This typically happens at radii between 100 and 150 AU from the central

¹ Supplementary content like movies from our calculations can be downloaded from the AIfA download page, <http://www.astro.uni-bonn.de/~webaiub/german/downloads.php>

TABLE 1
CALCULATIONS SUMMARY

Model	$N/1000$	M_* (M_\odot)	M_d (M_\odot)	M_{pert} (M_\odot)	r_{peri} (AU)	e	i (deg)	$m_{\text{env pert}}$ (M_J)	N_{formed}	N_{ejected}	Binaries?
E002	100	1.00	0.50	0.50	500	1.1	10	11.7	4	1	—
X002	250	1.00	0.50	0.50	500	1.1	10	12.0	5	2	1 (≈ 4 AU)
Y002	250	1.00	0.50	0.50	500	1.1	10	10.2	3	—	—
E003	100	0.75	0.48	0.50	500	1.1	10	16.1	3	2	1 (≈ 2 AU)
X003	250	0.75	0.48	0.50	500	1.1	10	12.6	4	1	—
E004	100	0.75	0.48	0.50	500	1.5	10	5.6	2	—	—
X004	100	0.75	0.48	0.50	500	1.5	10	11.0	3	—	—
E006	100	0.75	0.48	0.50	500	2.0	10	4.8	2	—	—
X006	250	0.75	0.48	0.50	500	2.0	10	4.4	3	—	1 (≈ 4 AU)
E007	100	0.75	0.48	0.50	500	3.0	10	2.1	0	—	—
E008	100	0.75	0.48	0.50	600	1.5	10	2.8	0	—	—
F008	100	0.75	0.48	0.50	600	1.1	10	6.5	0	—	—
E009	100	0.75	0.48	0.50	500	1.5	30	3.0	3	—	—
X009	250	0.75	0.48	0.50	500	1.5	30	7.6	4	—	1
E010	100	0.75	0.48	0.50	550	1.5	10	4.1	3	—	—
X010	250	0.75	0.48	0.50	550	1.5	10	8.8	4	—	—
E011	100	0.75	0.48	0.50	500	1.5	45	7.6	6	—	—
F011	100	0.75	0.48	0.50	500	1.5	45	4.2	2	—	—
X011	250	0.75	0.48	0.50	500	1.5	45	6.1	2	—	—
E015	100	0.75	0.48	0.40	400	1.5	45	7.9	3	—	—
E016	100	0.75	0.48	0.30	400	1.5	30	10.4	2	—	—
Total $N = 100\,000$ (10 of 13 models showing fragmentation):									30	3	1
Total $N = 250\,000$ (8 of 8 modes showing fragmentation):									28	3	3
Grand total (18 of 21 models showing fragmentation):									58	6	4

NOTE. — Overview of our SPH computations. The columns (from left to right) show the computation ID, the number of gas particles in thousands, the mass of the central star, its disc and the perturber star. Then follows the periastron distance of the encounter, the eccentricity and inclination. The four rightmost columns show the amount of gas captured by the perturber in a circumstellar envelope within a radius 40 AU, the number of formed companions in total and the number of bodies that got ejected during the calculation as well as the number of binary systems. In all models except for E015 and E016 the perturbing star has $0.5 M_\odot$ and passes the central star on an initially hyperbolic orbit with initial eccentricity between 1.1 and 3.0 and inclination to the disc plane between 10° and 45° .

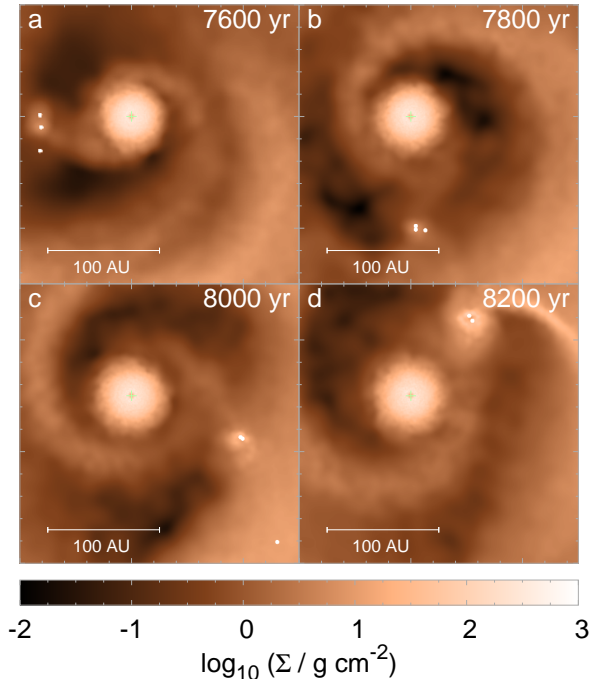


FIG. 3.— Snapshots of a forming binary around about 8000 years after the fly-by in model X002 (see also Figure 2). The components of the remaining VLMS pair have masses of $0.08 M_\odot$ and $0.09 M_\odot$, subsequently accreting another $0.01 M_\odot$ each. The escaping third body has $0.05 M_\odot$ and is eventually ejected.

star with some clumps forming even around 200 AU. Temporary overdensities do also occur within less than 100 AU but, however, dissolve quickly. This is probably due to the heat-

ing from the central star and the less effective cooling in these regions as already being mentioned in the Introduction and by Whitworth & Stamatellos (2006); Goodwin & Whitworth (2007). At radii larger than about 200 AU, on the other hand, the gas density is apparently too low for gravitationally bound clumps to form.

Each of the calculations typically produces between two and five (six on one case) low-mass objects with masses between those of very massive planets ($0.01 M_\odot$) and very low-mass stars ($0.13 M_\odot$). Additionally, mass is accreted onto the central star, and also mass is transferred to the perturber during the encounter. In the model shown in Figure 2 five objects with masses between $0.013 M_\odot$ and $0.10 M_\odot$ form; two of them being bound in a binary system. In addition, $0.016 M_\odot$ of gas accretes onto the central star within 15 000 years, and $0.0028 M_\odot = 2.8$ Jupiter masses (M_J) of gas transfers to the perturber (into the representing sink particle) while about $0.012 M_\odot (\approx 12 M_J)$ is captured around the perturber as a circumstellar envelope. In our analysis, any gas that is present within a radius of 40 AU but outside the sink radius is counted as circumstellar material of the perturber and shown in the ninth column of Table 1. This mass capture is typical, ranging between 2 and $16 M_J$.

In total, 28 bodies between 0.01 and $0.15 M_\odot$ formed in eight high resolution calculations, while the ten 100 000 particle calculations that showed fragmentation, yielded 30 bodies between 0.01 and $0.16 M_\odot$ (see Tables 1 and 2). Thus, there is no statistically significant relation between the resolution and the number of formed bodies. Similarly, no clear trend towards lower minimum masses of the companions for the high resolution can be derived from the current data. The average mass of the lowest-mass member is $0.056 M_\odot$ for the 100 000 particle models while it is $0.044 M_\odot$ for the 250 000 ones. Similarly, the average mass of the highest-

TABLE 2
OUTCOME OF INDIVIDUAL CALCULATIONS

100 000 particles			250 000 particles		
Model ID	m (M_{\odot})	Separation (AU)	Model ID	m (M_{\odot})	Sep. (AU)
E002			X002		
1	0.021	332–342	1	0.013	ejected
2	0.080	ejected	2	0.046	ejected
3	0.100	20–30	3	0.057	155–225
4	0.131	50–100	4a	0.088	70–110
			4b	0.099	70–110
E003			X003		
1a	0.013	130–500	1	0.021	50–100
1b	0.086	130–500	2	0.022	200
2	0.130	29–42	3	0.055	ejected
			4	0.154	130–200
E004			X004		
1	0.134	160–190	1	0.026	150–220
2	0.162	60–90	2	0.096	50–170
			3	1.032	25
E006			X006		
1	0.063	35–70	1a	0.033	150
2	0.154	120–220	1b	0.046	150
			2	0.148	60
E009			X009		
1	0.026	16	1	0.049	20
2	0.099	50	2	0.064	230
3	0.133	140	3	0.073	230
			4	0.138	60
E010			X010		
1	0.066	190	1	0.031	190
2	0.117	80	2	0.058	40
2	0.092	80	2	0.106	40
			3	0.128	80
E011			X011		
1	0.031	110	1	0.073	100–180
2	0.038	300	2	0.107	50–80
3	0.038	700			
4	0.048	230			
5	0.074	15–20			
6	0.098	125			
F011			Y002		
2	0.090	150–400	1	0.080	≈ 110
2	0.168	60–100	2	0.108	100–600
			3	0.137	≈ 50
Additional calculations with 100 000 particles					
E015			E016		
1	0.070	ejected	1	0.093	13–30
2	0.103	10–29	2	0.149	55–98
3	0.134	70–101			

NOTE. — List of the companions formed during individual calculations within 15 000–20 000 years after the flyby, sorted by mass. The table shows the masses and the approximate minimum and maximum separations from the central star. Note that bodies 4a and 4b in X002 got bound in a VLMS binary with a mutual distance of about 4 AU through a triple encounter while 1a and 1b in E003 got bound through dissipational capture. The binary capture of 1a and 1b in X006 probably involved both mechanisms.

mass is $0.097 M_{\odot}$ and $0.083 M_{\odot}$, respectively. Table 2 does also show the separations of the objects at the end of each calculation. It has to be noted that these can differ largely from the initial separation at the moment of formation. Dynamical interaction between the objects and the disc as well as mutual encounters push some bodies at wide and eccentric orbits or even eject them while others migrate closer to the star. The closest separation observed in our calculations is about 10 AU in model E015 after 15 000 years of evolution. The overall outcome is very similar to that of unperturbed self-fragmenting disc as shown in Stamatellos & Whitworth (2009b) except for the lower disc mass. This is quite plausible since the main difference between the two scenarios is the cause for the density patterns which undergo fragmenta-

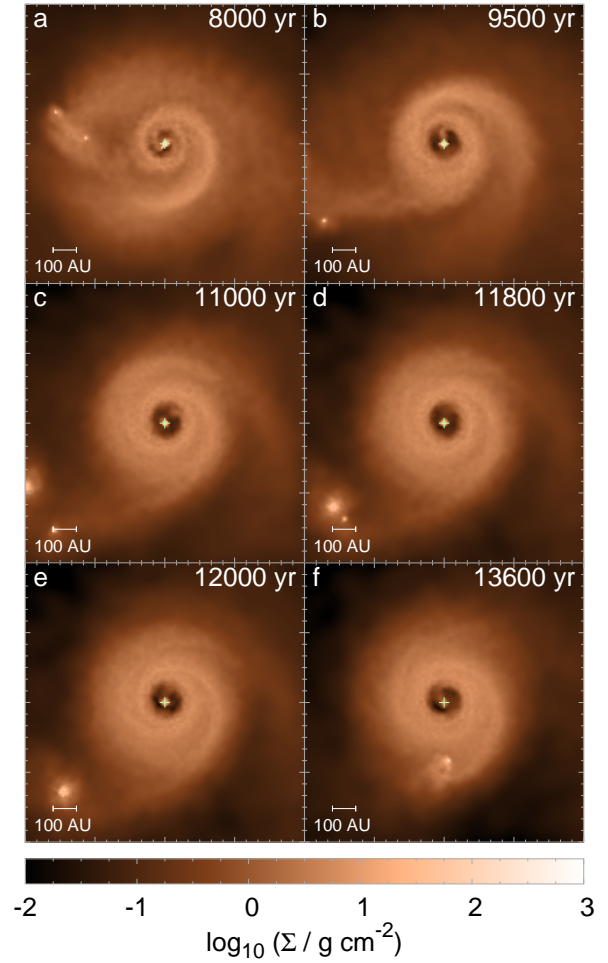


FIG. 4.— Snapshots of another forming binary around about 12000 years after the fly-by. The components of the remaining VLMS-BD pair have very unequal masses of $0.09 M_{\odot}$ and $0.013 M_{\odot}$ (with a mass ratio $q = 0.14$). In contrast to the binary formed in X002 (Figure 2) these bodies became bound due to a frictional encounter of their accretion envelopes.

tion. While Toomre density waves are the source of fragmentation in self-fragmenting discs, the gravitationally induced fragmentation occurs in tidal arms. In both cases, a dense bar-like in the disc reaches the density limit for fragmentation and thus the underlying physics is essentially the same.

Figure 5 shows the mass distribution of the n bodies created all calculations with 100 000 particles (top frame), 250 000 particles (middle frame) and both combined (bottom frame). A power law mass function $dn/dm = k(m/M_{\odot})^{-\alpha}$ can be fitted to this distribution. This has been done in this figure for the substellar regime (dashed line). In the bi-logarithmic scaling, the slope of $d \log n / d \log m$ corresponds to $1 - \alpha$ due to the differentiation of the logarithm (see Thies & Kroupa 2007 for details). The linear fit to the mass function for all calculation outputs combined appears to have a slope of $0.9^{+0.3}_{-0.4}$ ($< 0.16 M_{\odot}$) corresponding to power law index of $\alpha = -0.1^{+0.3}_{-0.4}$. If the calculations are separated by resolution, the 100 000 particle models correspond to $\alpha = +0.1^{+0.3}_{-1.5}$ while the 250 000 particle models similarly yield $\alpha = +0.1^{+0.3}_{-0.6}$. The slightly flatter IMF in the separate mass functions may be interpreted as a weak resolution-dependence of the average created mass which gets smeared out in the combined mass function. However, the difference between the slopes of 0.2 is within the

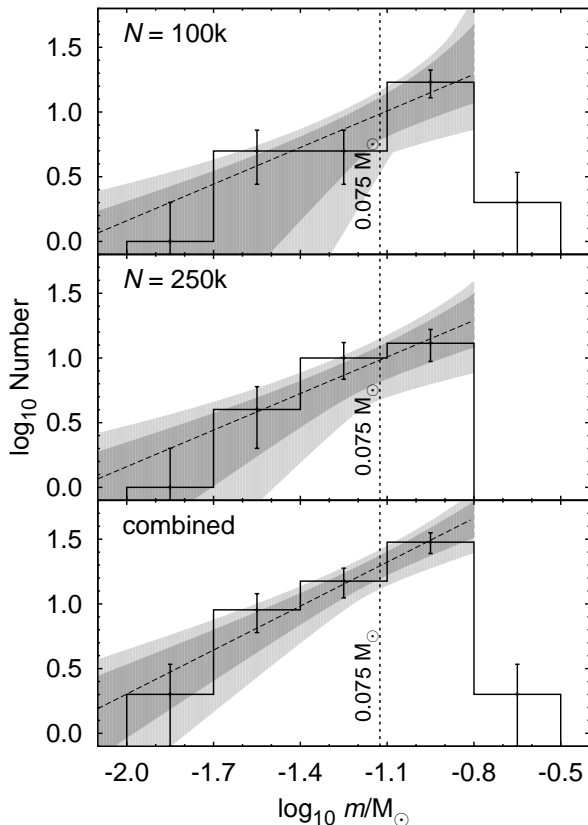


FIG. 5.— Mass distribution of the bodies created in the 100 000 particle models (top frame), the 250 000 particle models (middle frame), and both combined (bottom frame). The majority of companions is found in the mass interval between 0.08 and $0.16 M_{\odot}$ while most of the rest is in the substellar regime. The substellar mass function corresponds to a power law index of $\alpha = +0.1_{-1.5}^{+0.3}$ for the 100k models, $\alpha = +0.1_{-0.6}^{+0.3}$ for the 250k models, and $\alpha = -0.1_{-0.4}^{+0.3}$ for both combined (see text for further explanations). The dark and light grey-shaded regions refer to the 1 and 2σ confidence limits of the fit while the errorbars correspond to the 1σ Poisson errors. The vertical dotted line marks the hydrogen-burning mass limit of $0.075 M_{\odot}$ (Chabrier & Baraffe 2000).

1σ uncertainty The uncertainty, based on the Poisson errors of the log mass bins, is indicated by a shaded region. Above $0.12 M_{\odot}$ there is a sharp drop in the mass distribution that can be treated as a truncation. Similar results have been obtained by Stamatellos & Whitworth (2009a) and Shen et al. (2010). Interestingly, this is also in good agreement with both the sub-stellar IMF deduced by Kroupa (2001) as well as with the separate substellar IMF deduced in Thies & Kroupa (2007, 2008). However, more calculations are needed to provide statistically robust tests of the IMF. Furthermore, there is no weighting with respect to the different likelihood of the different encounter settings (i.e., inclination, fly-by distance etc.). Since the outcome of the computations does not show a specific dependency on the orbital parameters (except for whether there is fragmentation) such a weighting might introduce an artificial bias by amplifying the random noise of higher-weighted models.

4.2. Binary formation

In the same way as in the models of Stamatellos & Whitworth (2009a) of isolated circum-stellar discs, very low-mass binary systems can also form in gentle three-body encounters between low-mass objects

in the disc. Such a triple in-orbit encounter occurred during the X002 computation about 8,000 years after the fly-by, as shown in Figure 3 where a 4 AU binary system composed of $0.09 M_{\odot}$ and $0.10 M_{\odot}$ objects forms through a triple encounter. This binary remains bound to the host star in an orbit of about 100 AU. These separations are consistent with the observations of VLMS binaries according to which the most probable separation is around 3 AU (see, e.g., Figure 10 in Stamatellos & Whitworth 2009a). Another binary-forming mechanism was unveiled during calculation E003 (see Table 2). A 2 AU binary, consisting of a VLMS of $0.09 M_{\odot}$ and a BD with $0.013 M_{\odot}$, formed through a grazing encounter of circum-substellar accretion envelopes, which subsequently evolve into a circumbinary disc. The event is shown in a sequence plot in Figure 4. In two similar events in run X006, two accreting clumps merged to a single one of about $0.03 M_{\odot}$ 9600 yrs after the fly-by, and 6000 yrs later this body and a third one got captured into a binary of about 5 AU separation, probably involving both triple encounter and grazing collision. The masses at the end of the calculation are 0.03 and $0.04 M_{\odot}$.

Binaries formed via these processes may later be separated from their host star in a subsequent encounter with another star as already discussed for single substellar companions (Kroupa 1995; Goodwin & Whitworth 2007), or, possibly, by dynamical interaction with more massive companions in the same system. These models produce 55 systems of BDs and VLMSs, and 3 binaries giving a binary of $3/55 = 0.05$, whereby the binaries have semi-major axes of 4, 2 and 5 AU. Thus, while the separations are quite consistent with the observed VLMS and BD binaries, the present theoretical binary fraction is somewhat low.

4.3. The role of eccentricity and inclination

In a previous study (Thies et al. 2005) we found that the strength of the perturbation increases with decreasing eccentricity and inclination. This agrees with results of an SPH parameter study by Pfalzner et al. (2005). While disc-disc collisions produce most objects due to shock formation (Shen et al. 2010), coplanar encounters increase the effectiveness of the tidal perturbations which cause our discs to fragment. This is a consequence of the low relative velocity between the perturber and the perturber-facing parts of the disc in coplanar encounters, and thus a longer tidal exposure time. While drag forces in disc-disc collisions are larger for larger collisional velocities the tidal force does not depend on the velocity, and therefore the total amount of tidally transferred momentum for a given flyby distance is larger for slower encounters, i.e., for those with lower eccentricity.

5. DISCUSSION

Our computations show that the tidal perturbations of massive (otherwise stable) discs can form massive planets and BDs. Previous computations had assumed the interaction of two massive discs (Shen et al. 2010), reducing the probability of such an event dramatically. Our scenario only requires a single extended disc. This scenario can produce very low-mass companions at large distances from the primary star, and may help explain recent direct detections of massive planets orbiting at > 100 AU, far beyond where core accretion could have formed them², as well as intermediate (Liu et al. 2002) and distant (Stamatellos et al. 2007a;

² See also the Extrasolar Planets Encyclopaedia, <http://exoplanet.eu/>

Stamatellos & Whitworth 2009a) BD companions to stars. Like Stamatellos & Whitworth (2009a) we are also able to form BD binaries through three body encounters within the disc, and in addition, through dissipative encounters. But the required disc mass is considerably smaller, by about 30–40%, since even initially stable discs do fragment upon perturbation in our calculations. The mass function of companions formed by this process is in good agreement with that of self-fragmentation and with the separate substellar IMF deduced in Thies & Kroupa (2007). However, the volume of the current results does not allow robust statistical tests of the normalization of this sub-stellar IMF relative to the stellar IMF. Nevertheless, the obtained results are in remarkable agreement both with the form of the substellar IMF and the binary properties in the BD and VLMS regime, although the binary fraction is somewhat low (Section 4.2). More computations will have to be performed at different resolutions (up to a million particles) to enhance quantity as well as quality of the data.

5.1. How often do such encounters occur?

Furthermore, it has to be noted that triggered fragmentation is probably responsible only for a fraction of disc-fragmentation events while a good fraction may be triggered simply by over-feeding of an accreting disc towards self-fragmentation. Although the borders of the parameter subspace suitable for triggered fragmentation are not yet fully determined the current findings show that encounters of a higher inclination than 45 degrees, outside 600 AU or with eccentricities above 2 are generally unlikely to trigger fragmentation for the disc type studied here. The same holds true for perturbers of less than $0.3 M_{\odot}$.

By combining all these limits of the parameter space one can estimate the fraction of random encounters with a mutual periastron below 500 AU that are suitable for fragmentation of the analysed disc type. If a characteristic velocity dispersion of $\sim 2 \text{ km s}^{-1}$ and an upper stellar mass limit of $10 M_{\odot}$ within the host cluster is assumed only about 3% of all encounters below 500 AU lead to fragmentation. However, discs with even only slightly larger mass or lower background temperature may be pushed much easily to fragmentation, probably enlarging the parameter space significantly. Furthermore, other perturbing effects like stellar winds or supernova shock waves, which might influence large volumes within the host cluster at once, are not covered by this study, nor are the effects of dust.

5.2. Consequences for planet formation

All objects formed in our calculations have masses above $0.01 M_{\odot}$ or $10 M_J$ and are thus above the masses typically assumed for planets. However, we cannot rule out at the moment that also objects below $0.01 M_{\odot}$ may form through fragmentation, especially around lower-mass host stars which heat the inner disc region much less than more massive ones. Another critical point may be the resolution limits (although the local Jeans mass is well resolved even in the inner disc region, as discussed in Section 3.1).

It has to be emphasized, that planet formation probably typically takes place in the inner disc region through core-accretion (Hillenbrand 2008) which are less influenced by the perturbation unless companions formed through it migrate into these inner regions. There might still be significant impacts on the outcome of planet formation for stellar encounters, though. Even temporary gravitational instabilities that

do not collapse into a brown dwarf or planet directly may induce the formation of substellar companions down to Kuiper-Belt objects by induced vorticity and subsequent dust trapping (Barge & Sommeria 1995; Klahr & Bodenheimer 2003, 2006). Also the development of baroclinic vortices may be altered under the influence of tidal perturbations, either inhibiting or promoting the formation of dust aggregates. This mechanism may even work in typical protoplanetary discs and is subject of our ongoing research. According to solar system architecture (Heller 1993; Eggers et al. 1997; Kenyon & Bromley 2004) and radionuclide evidence (Takigawa et al. 2008; Sahijpal & Gupta 2009; Gaidos et al. 2009; Gounelle & Meibom 2008, however, disagree) the highly probable origin of our Sun in a large star-forming region further emphasizes the importance of such scenarios.

Another fact worth to be discussed is the capture of disc material by the perturbing star. As mentioned in Section 4 about $0.003 M_{\odot} = 3 M_J$ are accreted by the perturber in a typical 500 AU encounter like model E/X002, while the amount of accreted gas can be as large as $10 M_J$, as in models E/X003 (see Table 1). An even larger amount can be contained in a circumstellar disc or envelope around the perturber. Although being smaller than typically assumed for the Minimum-Mass Solar Nebular (MMSN, see Crida 2009) this may still be sufficient for the formation of Jupiter- or Saturn-type planets around the perturber. Since the orientation of this encounter-related accretion disc is not correlated to the stellar rotation of the perturber, this scenario may provide an explanation for highly inclined or even retrograde planets which have recently been detected (Narita et al. 2009; Johnson et al. 2009). If the captured gas is accreted onto a pre-existing circumstellar disc of the perturber star this might even lead to the formation of planetary systems with multiple mutually inclined (or even retrograde) orbital planes.

We have to emphasize at this point that gas capture from a massive extended circumstellar disc is only one of several possible gas capture scenarios, and is being observed in our work as a spin-off besides the main topic of this article. As the more general case, capture of material from any dense gas aggregate in the hosting star-forming region after the formation of the protostar itself may be a possible channel to form non-aligned planets. As the most general formulation, we note that the whole process of planet formation from the pre-stellar cloud in the context of stellar encounters in young star clusters to a fully established planetary system appears to be a discontinuous one in many cases, probably limiting the probability of regularly-shaped planetary systems with Solar system-like architecture. This issue will be investigated in detail in future work.

One issue not treated by our calculations is the varying protostar and disc mass during the accretion process. According to Machida et al. (2010) the growing disc may become temporarily unstable when the mass of the protostar is still negligibly small ($\sim 10^{-3} M_{\odot}$). In their nested-grid calculations, the disc fragments in the region of < 100 AU, and even within 10 AU. However, their simulations do not include a realistic treatment of radiative transfer. It is subject to future investigations whether accreting discs under perturbation may develop into planetary systems with Solar-type architecture.

Furthermore, the influence of magnetic fields are completely ignored in our calculations. Liverts et al. (2010) show that both hydromagnetic and thermomagnetic effects may amplify density waves in the disc into instability, and may pro-

vide an effective viscosity via turbulence which may assist accretion onto the star.

Observations of tidally perturbed fragmenting discs would surely be the best confirmation of this scenario. Due to the short duration of the flyby of only about 10,000 years the chance of such an event to be 'caught in the act' is small. It may, however, be possible to identify encounter-triggered fragmentation if observers succeed in detecting the typical tidal arms around the disc-hosting star as well as smaller amounts of non-circular filaments around a close-by star indicating it as a candidate perturber star. Such structures may be detectable with future high-resolution instruments like ALMA in star-forming regions like the ONC. Another possibility is to target FU Orionis stars which are thought to be undergoing enhanced accretion, such enhanced accretion may be caused by the perturbation of discs by a close encounter.

6. SUMMARY AND CONCLUSIONS

In a series of SPH calculations we have shown that massive ($\sim 0.5 M_{\odot}$), extended (≥ 100 AU) circumstellar discs can be stable when isolated, but fragment when perturbed by a moderately close and slightly inclined stellar encounter. Binaries formed in two cases via triple encounters of companions and via grazing encounters of accreting envelopes. This agrees with binary formation in self-fragmenting discs (Stamatellos & Whitworth 2009a). We further found that the

mass distribution of companions formed in discs is in agreement with the canonical substellar IMF as a separate population (Kroupa 2001; Kroupa & Bouvier 2003; Thies & Kroupa 2007, 2008). We have, however, to note that direct tidally induced fragmentation is probably only responsible for a fraction of all disc fragmentation events due to the relatively small orbital parameter subset that is suitable for fragmentation of discs of about $0.5 M_{\odot}$. More massive discs are expected to be more prone to fragmentation even due to weak perturbations, but are also more likely to reach the limit for self-fragmentation. This study, however, shows that tidal perturbations do not necessarily inhibit fragmentation but are instead capable of inducing fragmentation in disc that otherwise would silently disperse or be accreted by the central star without ever experiencing fragmentation. The perturber star may accrete gas from the target circumstellar disc and may form planets on misaligned or even counter-rotating orbits with respect to the stellar spin. Future work will analyse discs with different masses and more or less massive host stars as well.

ACKNOWLEDGEMENTS

This work was partially supported by the University of Bonn and partially by DFG grant KR1635/12-1. IT wishes to thank Dr. Sambaran Banerjee and Dr. Ole Marggraf for their kind assistance in improving this paper.

REFERENCES

- Barge, P., & Sommeria, J. 1995, *A&A*, 295, L1
 Bell, K. R., & Lin, D. N. C. 1994, *ApJ*, 427, 987
 Black, D. C., & Bodenheimer, P. 1975, *ApJ*, 199, 619
 Boffin, H. M. J., Watkins, S. J., Bhattal, A. S., Francis, N., & Whitworth, A. P. 1998, *MNRAS*, 300, 1189
 Boley, A. C., Hartquist, T. W., Durisen, R. H., & Michael, S. 2007, *ApJ*, 656, L89
 Boss, A. P. 1997, *Science*, 276, 1836
 —. 2004, *ApJ*, 610, 456
 —. 2006, *ApJ*, 641, 1148
 Boss, A. P., & Bodenheimer, P. 1979, *ApJ*, 234, 289
 Boss, A. P., & Myhill, E. A. 1992, *ApJS*, 83, 311
 Cai, K., Pickett, M. K., Durisen, R. H., & Milne, A. M. 2010, *ApJ*(accepted)
 Chabrier, G., & Baraffe, I. 2000, *ARA&A*, 38, 337
 Commerçon, B., Hennebelle, P., Audit, E., Chabrier, G., & Teyssier, R. 2008, *A&A*, 482, 371
 Crida, A. 2009, *ApJ*, 698, 606
 Eggers, S., Keller, H. U., Kroupa, P., & Markiewicz, W. J. 1997, *Planet. Space Sci.*, 45, 1099
 Eisner, J. A., & Carpenter, J. M. 2006, *ApJ*, 641, 1162
 Forgan, D., & Rice, K. 2009, *MNRAS*, 400, 2022
 Gaidos, E., Krot, A. N., Williams, J. P., & Raymond, S. N. 2009, *ApJ*, 696, 1854
 Goodwin, S. P., & Whitworth, A. 2007, *A&A*, 466, 943
 Goodwin, S. P., Whitworth, A. P., & Ward-Thompson, D. 2004, *A&A*, 414, 633
 Gounelle, M., & Meibom, A. 2008, *ApJ*, 680, 781
 Heller, C. H. 1993, *ApJ*, 408, 337
 Henning, T. 2008, *Physica Scripta Volume T*, 130, 014019
 Hillenbrand, L. A. 2008, *Physica Scripta Volume T*, 130, 014024
 Hubber, D. A., Goodwin, S. P., & Whitworth, A. P. 2006, *A&A*, 450, 881
 Hubeny, I. 1990, *ApJ*, 351, 632
 Johnson, J. A., Winn, J. N., Albrecht, S., Howard, A. W., Marcy, G. W., & Gazak, J. Z. 2009, *PASP*, 121, 1104
 Kenyon, S. J., & Bromley, B. C. 2004, *Nature*, 432, 598
 Klahr, H., & Bodenheimer, P. 2003, *ApJ*, 582, 869
 —. 2006, *ApJ*, 639, 432
 Kroupa, P. 1995, *MNRAS*, 277, 1491
 —. 2001, *MNRAS*, 322, 231
 —. 2005, *Nature*, 434, 148
 Kroupa, P., Aarseth, S., & Hurley, J. 2001, *MNRAS*, 321, 699
 Kroupa, P., & Bouvier, J. 2003, *MNRAS*, 346, 369
 Kroupa, P., Bouvier, J., Duchêne, G., & Moraux, E. 2003, *MNRAS*, 346, 354
 Liu, M. C., Fischer, D. A., Graham, J. R., Lloyd, J. P., Marcy, G. W., & Butler, R. P. 2002, *ApJ*, 571, 519
 Liverts, E., Mond, M., & Urpin, V. 2010, *MNRAS*, 404, 283
 Lodato, G., Meru, F., Clarke, C. J., & Rice, W. K. M. 2007, *MNRAS*, 374, 590
 Machida, M. N., Inutsuka, S., & Matsumoto, T. 2010, *ApJ*(submitted)
 Masunaga, H., & Inutsuka, S. 2000, *ApJ*, 531, 350
 Masunaga, H., Miyama, S. M., & Inutsuka, S. 1998, *ApJ*, 495, 346
 Mayer, L., Quinn, T., Wadsley, J., & Stadel, J. 2002, *Science*, 298, 1756
 Narita, N., Sato, B., Hirano, T., & Tamura, M. 2009, *PASJ*, 61, L35
 Nelson, A. F. 2006, *MNRAS*, 373, 1039
 Papaloizou, J. C. B., & Terquem, C. 2006, *Reports on Progress in Physics*, 69, 119
 Pfalzner, S., Vogel, P., Scharwächter, J., & Olczak, C. 2005, *A&A*, 437, 967
 Sahijpal, S., & Gupta, G. 2009, *Meteoritics and Planetary Science*, 44, 879
 Shen, S., Wadsley, J., Hayfield, T., & Ellens, N. 2010, *MNRAS*, 401, 727
 Spiegel, E. A. 1957, *ApJ*, 126, 202
 Stamatellos, D., Hubber, D. A., & Whitworth, A. P. 2007a, *MNRAS*, 382, L30
 Stamatellos, D., & Whitworth, A. P. 2008, *A&A*, 480, 879
 —. 2009a, *MNRAS*, 392, 413
 —. 2009b, *MNRAS*, 400, 1563
 Stamatellos, D., Whitworth, A. P., Bisbas, T., & Goodwin, S. 2007b, *A&A*, 475, 37
 Takigawa, A., Miki, J., Tachibana, S., Huss, G. R., Tominaga, N., Umeda, H., & Nomoto, K. 2008, *ApJ*, 688, 1382
 Thies, I., & Kroupa, P. 2007, *ApJ*, 671, 767
 —. 2008, *MNRAS*, 390, 1200
 Thies, I., Kroupa, P., & Theis, C. 2005, *MNRAS*, 364, 961
 Toomre, A. 1964, *ApJ*, 139, 1217
 Watkins, S. J., Bhattal, A. S., Boffin, H. M. J., Francis, N., & Whitworth, A. P. 1998a, *MNRAS*, 300, 1205
 —. 1998b, *MNRAS*, 300, 1214
 Whitehouse, S. C., & Bate, M. R. 2006, *MNRAS*, 367, 32
 Whitworth, A. P., & Stamatellos, D. 2006, *A&A*, 458, 817